ELSEVIER

Journal of Organometallic Chemistry 652 (2002) 37–49

Journal of Organometallic Chemistry

www.elsevier.com/locate/jorganchem

The syntheses and structures of coordinatively unsaturated aryloxy-hydride complexes of molybdenum, $Mo(PMe_3)_4(OAr)H$: reversible C–H bond activation and comparison with their tungsten analogues

Tony Hascall, Vincent J. Murphy, Kevin E. Janak, Gerard Parkin *

Department of Chemistry, Columbia University, 3000 Broadway (Box 3115), New York, NY 10027, USA

Received 13 November 2001

Abstract

$Mo(PMe_3)_6$ reacts with ArOH (Ar = 2,4,6-$C_6H_2Me_3$, 2,6-$C_6H_3Pr^i_2$) to give coordinatively unsaturated aryloxy-hydride derivatives $Mo(PMe_3)_4(OAr)H$. The formation of $Mo(PMe_3)_4(OAr)H$ is in marked contrast to the cyclometalated products of C–H bond activation that are obtained for the corresponding tungsten system. Deuterium labeling and magnetization transfer studies, however, demonstrate that the coordinatively unsaturated molybdenum complexes $Mo(PMe_3)_4(OAr)H$ are in fact kinetically capable of intramolecular oxidative addition of a C–H bond of the *ortho* substituents to yield cyclometalated derivatives that are thermodynamically unstable with respect to the aryloxy-hydride derivatives. © 2002 Published by Elsevier Science B.V.

Keywords: Molybdenum; Tungsten; Trimethylphosphine; Aryloxy; Hydride; Carbon–hydrogen bond cleavage

1. Introduction

The reactivity of carbon–hydrogen bonds towards transition metals continues to be an important area of research due to its relevance to the selective functionalization of hydrocarbons [1]. We are particularly interested in the chemistry of electron-rich transition metal complexes due to their potential to react with a variety of bonds by oxidative-addition. For example, previous studies have demonstrated that $W(PMe_3)_6$ and $W(PMe_3)_4(\eta^2\text{-}CH_2PMe_2)H$ react with the carbon–hydrogen bonds of alcohols. Thus, $W(PMe_3)_4(\eta^2\text{-}CH_2PMe_2)H$ reacts with MeOH to give an η^2-formaldehyde complex [2], while phenol derivatives react to give four- and five-membered oxametallacycles [3], as illustrated in Schemes 1 and 2 [4]. Most noteworthy of the latter reactions is the selectivity towards the formation of four-membered rings [3]. Since it is important to expand our understanding of the factors that promote C–H bond activation, we sought to compare analogous reactions of the molybdenum counterpart $Mo(PMe_3)_6$ [5]. Significantly, the chemistry of these molybdenum and tungsten systems proved to be quite distinct with respect to their ability to achieve C–H bond activation [6].

2. Results and discussion

2.1. Reactivity of $Mo(PMe_3)_6$ towards methanol: C–H bond activation and the synthesis of the formaldehyde complex $Mo(PMe_3)_4H_2(\eta^2\text{-}CH_2O)$

The reaction of $Mo(PMe_3)_6$ with methanol in pentane results in the oxidative addition of both an O–H and C–H bond to give the formaldehyde complex $Mo(PMe_3)_4H_2(\eta^2\text{-}CH_2O)$, as illustrated in Scheme 1, analogous to the synthesis of the tungsten complex $W(PMe_3)_4H_2(\eta^2\text{-}CH_2O)$ by reaction of $W(PMe_3)_4(\eta^2\text{-}CH_2PMe_2)H$ with methanol [2]. A related Mo formaldehyde complex, $(dppe)_2MoH_2(\eta^2\text{-}CH_2O)$, has recently been reported to be formed from the decomposition of $(dppe)_2MoH_2(OMe)_2$ [7,8]. The formaldehyde ligand of $Mo(PMe_3)_4H_2(\eta^2\text{-}CH_2O)$ is characterized by a singlet in the ^{1}H-NMR spectrum at δ 3.51 and a triplet in the ^{13}C-NMR spectrum at δ 63.4 ($^1J_{C-H} = 159$ Hz) [9]. Further-

* Corresponding author.
E-mail address: parkin@chem.columbia.edu (G. Parkin).

0022-328X/02/$ - see front matter © 2002 Published by Elsevier Science B.V.
PII: S0022-328X(02)01306-2

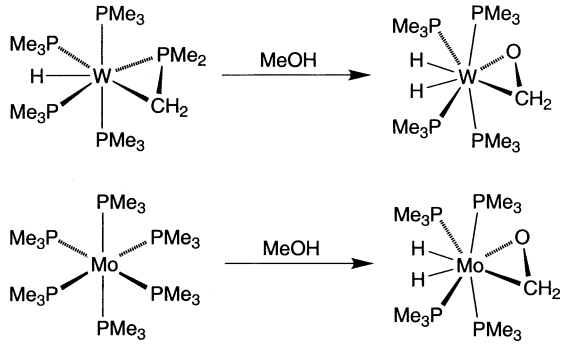

Scheme 1.

more, the hydride ligands are observed as a quintet in the ^{1}H-NMR spectrum at δ −2.65 ($^2J_{P-H} = 38$ Hz).

The molecular structure of $Mo(PMe_3)_4H_2(\eta^2\text{-}CH_2O)$ has been determined by X-ray diffraction (Fig. 1), confirming the η^2-coordination mode of the formaldehyde ligand moiety. However, the formaldehyde and hydride ligands are disordered so that detailed discussion of the bonding is unwarranted.

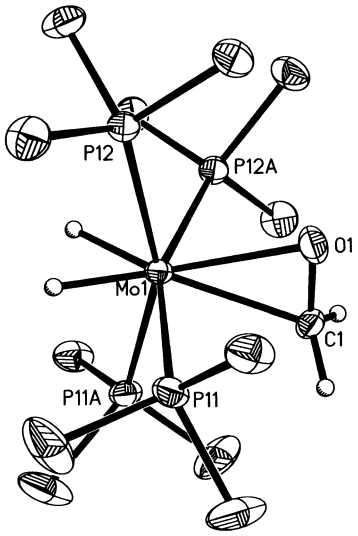

Fig. 1. Molecular structure of $Mo(PMe_3)_4H_2(\eta^2\text{-}CH_2O)$. Only one of the disordered conformations is shown.

2.2. Reactivity of $Mo(PMe_3)_6$ towards phenols: aryloxide formation without C–H bond activation

While the molybdenum and tungsten systems behave similarly with respect to the reactions with methanol, the reactions with phenols differ considerably. For example, $Mo(PMe_3)_6$ reacts with phenol to give the orange paramagnetic [10] *tetrakis*(phenoxide) complex $Mo(PMe_3)_2(OPh)_4$ (Scheme 3), in contrast to the diamagnetic yellow metallacycle $W(PMe_3)_4H_2(\eta^2\text{-}OC_6H_4)$ observed for the tungsten system (Scheme 2) [3]. Thus, in striking contrast to the tungsten system which achieves C–H bond activation, the molybdenum system is inert to the aryl C–H bonds of phenol. The molecular structure of $Mo(PMe_3)_2(OPh)_4$ has been determined by X-ray diffraction, as illustrated in Fig. 2. Also in contrast to the tungsten system, the formation of $Mo(PMe_3)_2(OPh)_4$ involves elimination of H_2. Precedence for such a reaction is, nevertheless, provided by the observation that $W(PMePh_2)_4Cl_2$ reacts with phenol or *p*-cresol to give $W(PMePh_2)_2Cl_2(OAr)_2$ and H_2 [11].

In an effort to achieve C–H bond activation by the molybdenum system, it was considered essential to prevent the formation of a *tetrakis*(aryloxy) derivative $Mo(PMe_3)_2(OAr)_4$ by using bulky substituents in the *ortho* positions to restrict the reaction of $Mo(PMe_3)_6$ to a single equivalent of the phenol. Indeed, $Mo(PMe_3)_6$ was observed to react with 2,4,6-trimethylphenol and

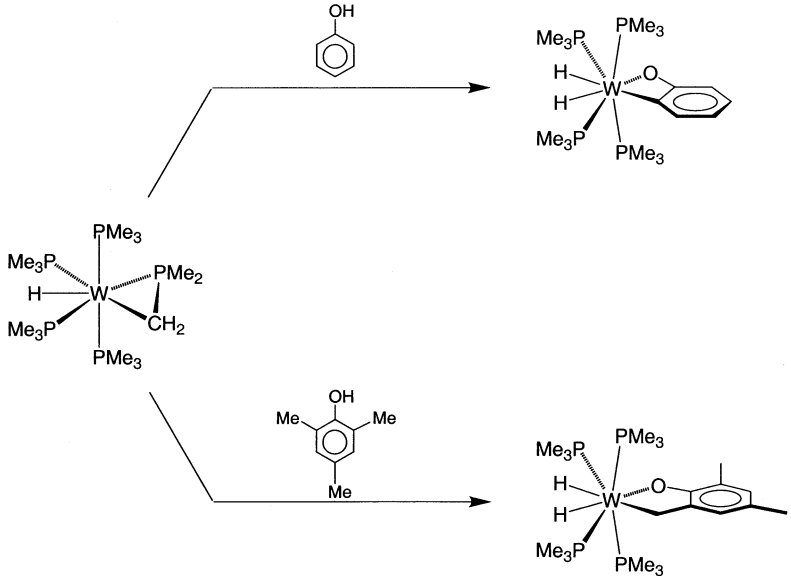

Scheme 2.

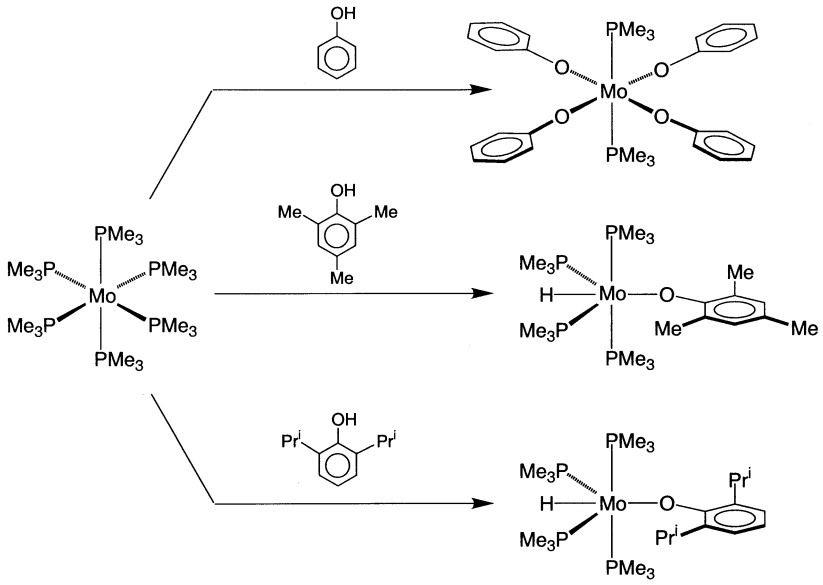

Scheme 3.

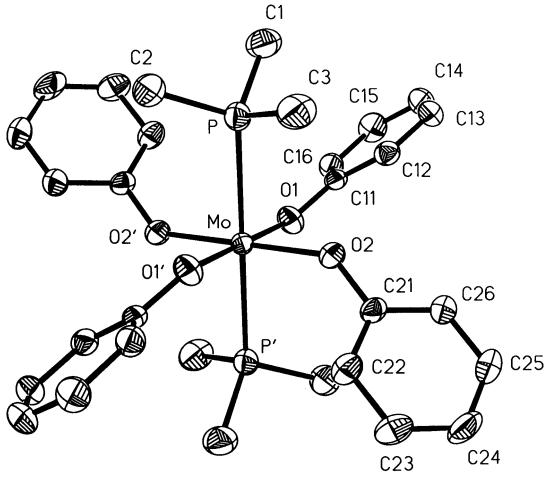

Fig. 2. Molecular structure of $Mo(PMe_3)_2(OPh)_4$. Selected bond lengths (Å) and angles (°): Mo–P 2.644(2), Mo–O(1) 1.966(3), Mo–O(2) 1.958(3); P–Mo–O(1) 97.8(1), P–Mo–O(2) 85.8(1), O(1)–Mo–O(2) 90.2(1), P–Mo–P′ 180.0; O(1)–Mo–P′ 82.2(1), O(2)–Mo–P′ 94.2(1), O(1)–Mo–(O1′) 180.0, O(2)–Mo–(O2′) 180.0, Mo–O(1)–C(11) 14.3(3), Mo–O(2)–C(21) 137.4(3).

2,6-diisopropylphenol to give the purple diamagnetic complexes $Mo(PMe_3)_4(OC_6H_2Me_3)H$ and $Mo(PMe_3)_4(OC_6H_3Pr^i_2)H$, respectively (Scheme 3). Mononuclear aryloxy-hydride complexes of Mo are not common and structurally characterized examples appear to be limited to the 18-electron complexes $[\eta^6,\eta^1\text{-}C_6H_5C_6H_3\text{-}(Ph)O]Mo(PMe_3)_2H$ [12] and $[\eta^6,\eta^1\text{-}C_6H_5C_6H_3(Ph)O]\text{-}Mo(PMePh_2)_2H$ [13], and the catecholate derivative $Mo(dppe)_2H_2(\eta^2\text{-}O_2C_6H_4)$ [7]. Related 18-electron octahedral $M(PMe_3)_4(OAr)H$ complexes are also known for ruthenium [14,15].

Decisive characterization of the products as aryloxy-hydride complexes, $Mo(PMe_3)_4(OC_6H_2Me_3)H$ and $Mo(PMe_3)_4(OC_6H_3Pr^i_2)H$, is provided by NMR spectroscopy. For example, the ^{1}H-NMR spectra of $Mo(PMe_3)_4(OC_6H_2Me_3)H$ and $Mo(PMe_3)_4(OC_6H_3Pr^i_2)H$ exhibit triplet of triplet resonances at δ −6.59 ($^2J_{P-H} = 23$ and 84 Hz) and −6.53 ($^2J_{P-H} = 22$ and 85 Hz) attributable to the Mo–H ligands, respectively. In addition to the integration of the ^{1}H-NMR spectra, evidence that the compounds are monohydrides, rather than 18-electron trihydrides $Mo(PMe_3)_4(OAr)H_3$, is provided by comparison of the fully $^{31}P\{^1H\}$ and selectively decoupled $^{31}P\{^1H\text{–}P(CH_3)_3\}$ spectra. Specifically, the latter spectra exhibit an additional doublet coupling, thereby providing convincing evidence that each complex contains only a single Mo–H ligand.

Additional characterization of $Mo(PMe_3)_4(OC_6H_2\text{-}Me_3)H$ and $Mo(PMe_3)_4(OC_6H_3Pr^i_2)H$ is provided by X-ray diffraction, with the molecular structures being illustrated in Figs. 3 and 4. Neglecting the hydride ligand, the coordination environment about molybdenum is based on a trigonal bipyramid, with axial PMe_3 ligands. The hydride ligands were observed in electron density difference maps and are located close to the equatorial plane and *trans* to the aryloxy substituent. This *trans* arrangement of the aryloxy and hydride ligands contrasts with the *cis* geometries observed for the related 18-electron octahedral complexes $Ru(PMe_3)_4(OC_6H_4Me)H$ [14] and $[Ir(PMe_3)_4(OMe)H][PF_6]$ [16]. While the position of hydrogen atoms determined by X-ray diffraction, particularly those bound to heavy metals, is subject to considerable uncertainty, the location of the hydride ligand *trans* to the aryloxy group in $Mo(PMe_3)_4(OAr)H$ is reasonable based on the arrangement of the other ligands. To illustrate this

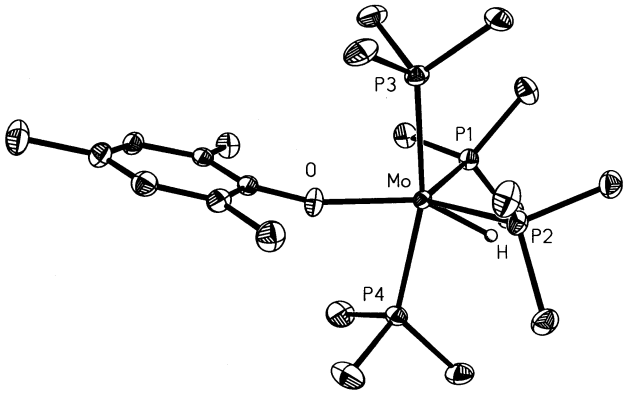

Fig. 3. Molecular structure of $Mo(PMe_3)_4(OC_6H_2Me_3)H$. Selected bond lengths (Å) and angles (°): Mo–P(1) 2.337(1), Mo–P(2) 2.348(1), Mo–P(3) 2.455(1), Mo–P(4) 2.473(1), Mo–O 2.065(3); P(1)–Mo–P(2) 109.3(1), P(1)–Mo–P(3) 88.9(1), P(2)–Mo–P(3) 88.4(1), P(1)–Mo–P(4) 97.4(1), P(2)–Mo–P(4) 101.4(1), P(3)–Mo–P(4) 165.7(1), P(1)–Mo–O 121.2(1), P(2)–Mo–O 129.0(1), P(3)–Mo–O 86.1(1), P(4)–Mo–O 79.6(1), Mo–O–C(1) 159.7(3).

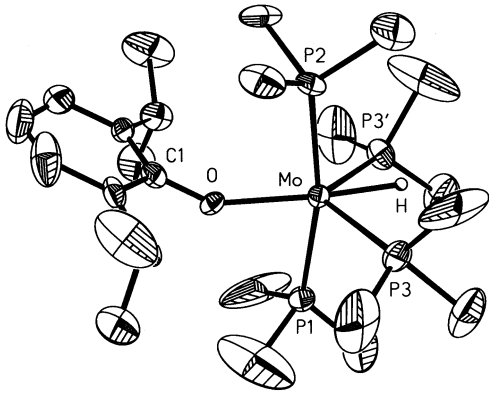

Fig. 4. Molecular structure of $Mo(PMe_3)_4(OC_6H_3Pr^i_2)H$. Selected bond lengths (Å) and angles (°): Mo–P(1) 2.460(3), Mo–P(2) 2.464(3), Mo–P(3) 2.338(2), Mo–O 2.072(6); P(1)–Mo–P(2) 168.4(1), P(1)–Mo–P(3) 90.4(1), P(2)–Mo–P(3) 96.3(1), P(1)–Mo–O 79.1(2), P(2)–Mo–O 89.3(2), P(3)–Mo–O 124.9(1), P(3)–Mo–P(3′) 108.9(1), Mo–O–C(1) 145.9(6).

point, the coordination environments of the metal centers in $Mo(PMe_3)_4(OC_6H_2Me_3)H$ and $Ru(PMe_3)_4(OC_6H_4Me)H$ (in which the hydride ligand was not located) [14a,14b] are compared in Fig. 5, from which it is evident that the coordination site for the hydride ligand is *trans* to the aryloxy ligand in the former complex, and *cis* in the latter species. In addition to the structural evidence, spectroscopic evidence that the hydride ligands of $Mo(PMe_3)_4(OC_6H_2Me_3)H$ and $Mo(PMe_3)_4(OC_6H_3Pr^i_2)H$ are best described as *trans* to an aryloxy rather than a PMe_3 ligand is provided by the observation that the hydride signals in the ^{1}H-NMR spectra do not exhibit the large *trans* $^2J_{P-H}$ couplings of ca. 100 and 145 Hz that are observed for $Ru(PMe_3)_4(OC_6H_4Me)H$ and $[Ir(PMe_3)_4(OMe)H][PF_6]$, respectively. It is worth noting that the structures of $Mo(PMe_3)_4(OAr)H$ are different from that of the

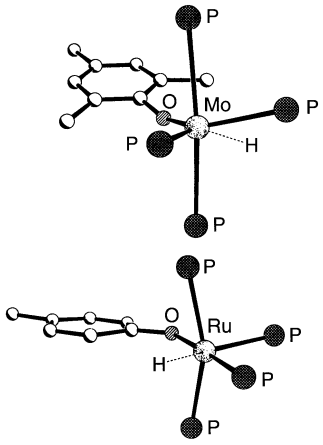

Fig. 5. Comparison of the molecular structures of $Mo(PMe_3)_4(OC_6H_2Me_3)H$ and $Ru(PMe_3)_4(OC_6H_4Me)H$ (for which the hydride ligand was not located) emphasizing the *trans* and *cis* aryloxy-hydride dispositions, respectively.

thiolate complex $Mo(dppe)_2(SC_6H_2Pr^i_3)H$ which has also been reported to adopt a *cis*-disposition of hydride and thiolate ligands, but the geometry is grossly distorted from octahedral [17].

The diamagnetic nature of the 16-electron d^4 $Mo(PMe_3)_4(OAr)H$ species is in contrast to related paramagnetic octahedral *trans*-$Mo(PMe_3)_4X_2$ (X = Cl, Br, I) complexes. A principal distinction between these two sets of complexes is that the four π-symmetry orbitals of the two *trans*-X atoms in $M(PMe_3)_4X_2$ belong to two sets of *E* symmetry orbitals (Fig. 6) [18]. As a consequence of this symmetry, the halide p-orbitals are required to interact with a *pair* of non-bonding metal orbitals (of the 't_{2g} set' in an idealized octahedral geometry), with the result that a d^4 metal center gives rise to a triplet. In contrast to *trans*-$Mo(PMe_3)_4X_2$, the π-donor orbitals of a single bent aryloxide ligand of $Mo(PMe_3)_4(OAr)H$ are not degenerate, and so it is permissible to interact with a single orbital of the 't_{2g} set' (Fig. 6) [19]. The result of this selective interaction with a single metal orbital is that the four non-bonding electrons fully occupy two d-orbitals and the compound is diamagnetic.

Evidence that lone pair π donation from oxygen is operative in $Mo(PMe_3)_4(OAr)H$ is provided by the observation that the Mo–OAr bond lengths are intermediate between those in the formally 14-electron complex $Mo(PMe_3)_2(OPh)_4$ and the 18-electron derivatives, $[\eta^6,\eta^1\text{-}C_6H_5C_6H_3(Ph)O]Mo(PMe_3)_2H$ and $[\eta^6,\eta^1\text{-}C_6H_5C_6H_3(Ph)O]Mo(PMePh_2)_2H$ [2.164(5) Å] [13] (Table 1). Thus, the Mo–O bond length increases with electron count, presumably as p_π–d_π donation from oxygen diminishes with increasing saturation of the metal center. Indeed, Rothwell has previously examined a series of tungsten chloro aryloxy complexes and found a good correlation between electron count and W–O bond length [20a]. The distances varied from 1.84 Å in

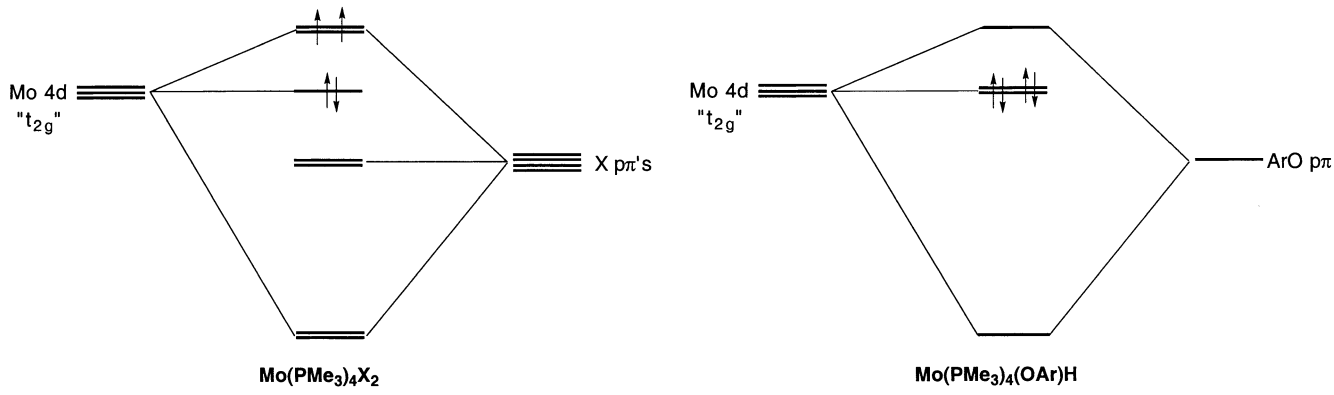

Fig. 6. Rationalization of the paramagnetic and diamagnetic natures of $Mo(PMe_3)_4X_2$ and $Mo(PMe_3)_4(OAr)H$.

12-electron *cis*-$WCl_4(OC_6H_3Ph_2)_2$ to 2.14 Å in 18-electron $[\eta^6,\eta^1$-$C_6H_5C_6H_3(Ph)O]W(dmpe)Cl$ and Rothwell concluded that the W–O bond length appears to be an excellent probe of the electronic demands of the metal center [20a]. Bond angles at oxygen, however, cannot alone be used reliably as an indicator of π-bonding, since they are also influenced by steric interactions [20].

2.3. Reversible C–H bond activation by molybdenum in the aryloxy-hydride complexes $Mo(PMe_3)_4(OAr)H$

2.3.1. Kinetics of C–H bond activation

The isolation of the molybdenum aryloxy-hydride complexes $Mo(PMe_3)_4(OAr)H$ is of particular significance since the tungsten analogues were postulated to be the intermediates responsible for the C–H bond activation reactions in the corresponding tungsten system. For example, $[W(PMe_3)_4(OC_6H_2Me_3)H]$ was proposed to be the intermediate that underwent intramolecular oxidative-addition of one of the *ortho*-methyl C–H bonds to give the five-membered oxametallacycle $W(PMe_3)_4[\eta^2$-$OC_6H_2Me_2(CH_2)]H_2$.

Although the 18-electron cyclometalated molybdenum complexes were not detected spectroscopically, evidence for their existence in equilibrium with $Mo(PMe_3)_4(OAr)H$ is provided by deuterium labeling and magnetization transfer studies. For example, scrambling of deuterium into the *ortho*-methyl groups of the mesityl ring is observed in the reaction of $Mo(PMe_3)_6$ with 2,4,6-$Me_3C_6H_2OD$ (Scheme 4) [21]. Incorporation of deuterium into the *ortho*-methyl groups of the mesityl ring may be rationalized by a mechanism that involves the reversible formation of a five-membered oxametallacycle-dihydride complex via sp^3 C–H bond activation, thereby permitting site exchange, as illustrated in Scheme 5 [22].

Reversible C–H bond activation within $Mo(PMe_3)_4(OAr)H$ is further demonstrated by ^{1}H-NMR magnetization transfer experiments [23] which demonstrate that exchange between the hydride and *ortho*-methyl groups of $Mo(PMe_3)_4(OC_6H_2Me_3)H$ is rapid on the NMR time-scale [24]. The magnetization transfer experiment also permits determination of the barrier for oxidative addition of the methyl C–H bond to the molybdenum center (Table 2 and Fig. 7): $\Delta H^{\ddagger} = 13.0(4)$ kcal mol^{-1} and $\Delta S^{\ddagger} = -8(2)$ e.u. [25].

Magnetization transfer studies were also performed on $Mo(PMe_3)_4(OC_6H_3Pr^i_2)H$, demonstrating exchange between both the methyl and methine protons of the isopropyl groups and the hydride group, indicating that both types of C–H bonds reversibly add to the metal (Scheme 6). However, because of the competing exchange mechanisms, the analysis of the data to obtain quantitative rate constant information is complex. Nevertheless, due to the fact that it was necessary to heat the sample to 340 K in order to observe magnetization transfer, it is evident that the barrier for oxidative addition of both types of the isopropyl C–H bonds is greater than that for the *ortho*-methyl groups of $Mo(PMe_3)_4(OC_6H_2Me_3)$, for which magnetization transfer was detected as low as 250 K.

Table 1
Mo–O bond lengths and Mo–O–C bond angles as a function of electron count

	Electron count	*d*(Mo–O) (Å)	Mo–O–C (°)	References
$Mo(PMe_3)_2(OPh)_4$	14	1.958(3), 1.966(3)	137.4(3), 141.3(3)	This work
$Mo(PMe_3)_4(OC_6H_2Me_3)H$	16	2.065(3)	159.7(3)	This work
$Mo(PMe_3)_4(OC_6H_3Pr^i_2)H$	16	2.072(6)	145.9(6)	This work
$[\eta^6,\eta^1$-$C_6H_5C_6H_3(Ph)O]Mo(PMe_3)_2H$	18	2.187(3)	118.3(3)	[a]

[a] T. Hascall, G. Parkin, unpublished results.

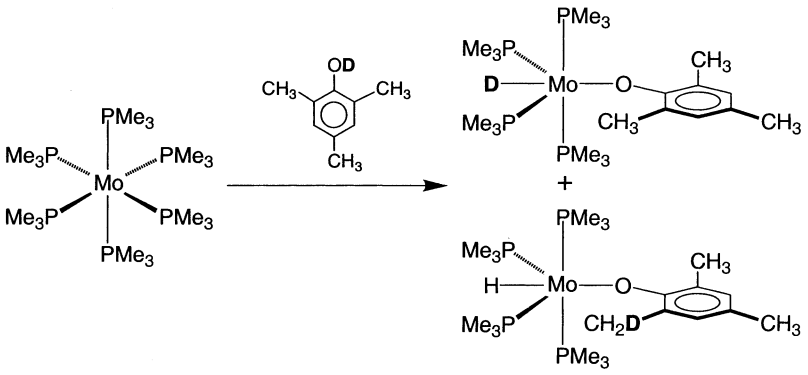

Scheme 4.

Table 2
Rate constants for intramolecular C–H bond activation of $Mo(PMe_3)_4(OC_6H_2Me_3)H$

Temperature (K)	k (s^{-1})
266	1.6
272	3.1
279	5.4
284	8.7
290	13.1
303	32.4
313	90.5

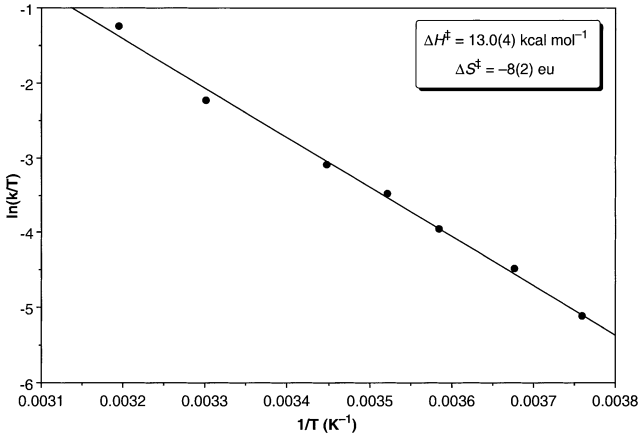

Fig. 7. Eyring plot for oxidative-addition of an *ortho* methyl C–H bond in $Mo(PMe_3)_4(OC_6H_2Me_3)H$.

2.3.2. Thermodynamics of C–H bond activation

The above deuterium labeling and magnetization transfer studies indicate that the six-coordinate aryloxy-hydride complexes $Mo(PMe_3)_4(OAr)H$ are kinetically capable of undergoing intramolecular C–H bond activation of the aryl substituents. As such, the inability to isolate the product of C–H bond activation implies that the process is not thermodynamically favored for molybdenum. The ability to isolate molybdenum species that correspond to reactive intermediates for tungsten is presumably a consequence of the fact that a second row transition metal typically forms weaker bonds to carbon and hydrogen than does the corresponding third row metal [26]. Consequently, the energy required to break the C–H bond is not compensated by the formation of Mo–C and Mo–H bonds [27]. Thus, for molybdenum, the equilibrium between the aryloxy derivative and its cyclometalated counterpart lies in favor of the former species, while for tungsten the latter prevails (Scheme 7). The relative energetics of these two equilibria resembles that of the cyclometalation equilibria involving $M(PMe_3)_6$ and $M(PMe_3)_4(\eta^2\text{-}CH_2PMe_2)H$, for which the equilibrium constant for the tungsten system is a factor of ca. 2×10^3 greater than that for molybdenum at 30 °C (Scheme 7) [5a,28].

In order to evaluate further the notion that the difference in the molybdenum and tungsten systems may be rationalized by the respective bond energies, a knowledge of their values is essential. Experimental data on metal–carbon and metal–hydrogen bond strengths are, however, relatively scarce [26]. Nevertheless, one system for which M–H and M–C bond energies have been measured for both Mo and W is Cp_2MH_2 and $Cp_2M(CH_3)_2$ [26b,29]. The bond energies for these complexes are listed in Table 3, from which it can be seen that the sum of the W–H and W–CH_3 bond strengths is considerably greater than that of Mo, by 26 kcal mol^{-1}. Thus, if the differences in M–H and M–C

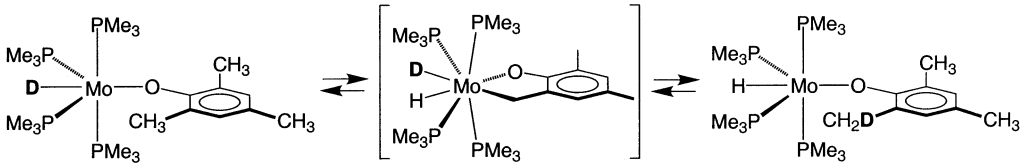

Scheme 5.

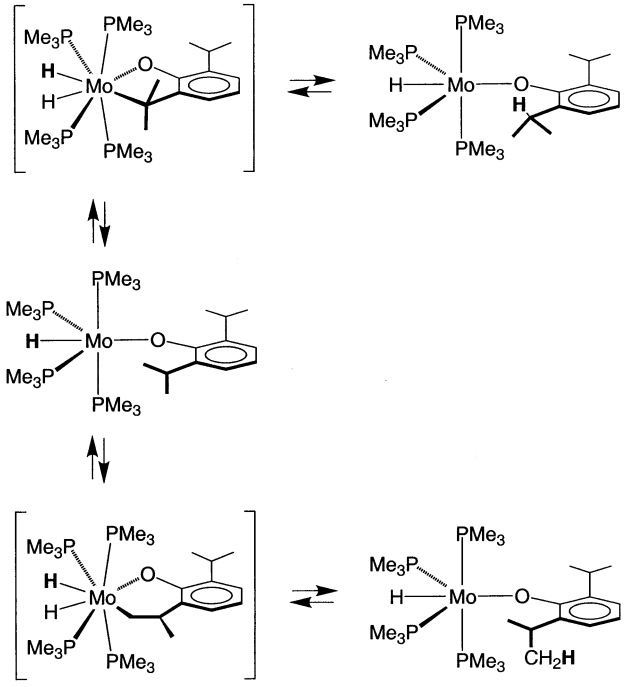

Scheme 6.

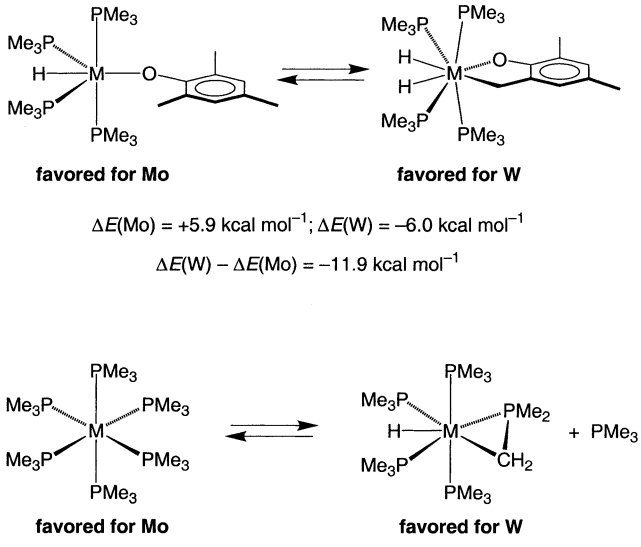

Scheme 7.

bond energies for the metallocene fragments translate to the Mo and W systems described here, intramolecular C–H bond activation formation would be predicted to be thermodynamically more favored for the tungsten system.

To provide a more quantitative evaluation and understanding of the energetics of these C–H bond activation reactions, we have performed DFT (B3LYP) calculations on $M(PMe_3)_4(OC_6H_2Me_3)H$ and

Table 3
M–H and M–C bond energies in Cp_2MH_2 and $Cp_2M(CH_3)_2$ (M = Mo, W) [a]

Bond energy (kcal mol^{-1})	Mo	W
D(M–C)	61	74
D(M–H)	40	53
D(M–H)+D(M–C)	101	127

[a] Data taken from: J.A. Martinho Simões, J.L. Beauchamp, Chem. Rev. 90 (1990) 629–688; M.J. Calhorda, A.R. Dias, M.E. Minas da Piedade, M.S. Salema, J.A. Martinho Simões, Organometallics 6 (1987) 734–738; A.R. Dias, J.A. Martinho Simões, Polyhedron 7 (1988) 1531–1544.

$M(PMe_3)_4H_2[\eta^2\text{-}OC_6H_2Me_2(CH_2)]$ (M = Mo, W). The optimized structures of $M(PMe_3)_4(OC_6H_2Me_3)H$ and $M(PMe_3)_4H_2(\eta^2\text{-}OC_6H_2Me_2CH_2)$ are similar for each metal and are comparable to the experimental structures of $Mo(PMe_3)_4(OC_6H_2Me_3)H$ and $W(PMe_3)_4H_2[\eta^2\text{-}OC_6H_2Me_2(CH_2)]$. Selected metrical data for the calculated structures are given in Tables 4 and 5, along with experimental data for comparison. From these data, it is evident that there is reasonable agreement between the calculated and experimental structures, although the DFT calculations systematically overestimate the metal–ligand bond lengths, as has been previously observed [30]. The relative energies [31] of the two isomers for each metal are given in Table 6, demonstrating that the calculations agree with the experimental observations that the aryloxy-hydride species is favored for Mo while the C–H bond activated isomer predominates for tungsten. In each case, the preferred isomer is favored by ca. 6 kcal mol^{-1}. Ignoring entropy changes, such an energy difference corresponds to an equilibrium constant of ca. 2×10^4 at 298 K, a value sufficiently large to explain why the disfavored isomers have not been observed spectroscopically for either system. If the strength of the *ortho* C–H bond of the aryloxy ligand is taken to be the same as the methyl C–H bond in toluene, 88 kcal mol^{-1} [32], then the calculated sum of the energies of the M–C and M–H bonds formed by the cyclometallation of $M(PMe_3)_4(OC_6H_2Me_3)H$ are 82 and 94 kcal mol^{-1} for Mo and W, respectively [33].

Table 4
Selected calculated metrical data for $M(PMe_3)_4(OC_6H_2Me_3)H$ (M = Mo, W); experimental values for $Mo(PMe_3)_4(OC_6H_2Me_3)H$ given in parentheses

	Mo	W
M–O (Å)	2.118 (2.065)	2.073
M–O–C (°)	150.0 (159.7)	151.5
M–H (Å)	1.743	1.751
M–P_{ax} (Å)	2.530 (2.455)	2.530
	2.549 (2.473)	2.529
M–P_{eq} (Å)	2.419 (2.337)	2.416
	2.418 (2.348)	2.417

Table 5
Selected calculated metrical data for $M(PMe_3)_4H_2[\eta^2\text{-}OC_6H_2Me_2(CH_2)]$ (M = Mo, W); experimental values for $W(PMe_3)_4H_2[\eta^2\text{-}OC_6H_2Me_2(CH_2)]$ given in parentheses

	Mo	W
M–O (Å)	2.195	2.176 (2.145)
M–C (Å)	2.333	2.327 (2.290)
M–H (Å)	1.720	1.738
	1.726	1.732
$M–P_{ax}$ (Å)	2.578	2.559 (2.494)
	2.571	2.571 (2.496)
$M–P_{eq}$ (Å)	2.582	2.493 (2.426)
	2.495	2.568 (2.479)

Table 6
Calculated energies (kcal mol^{-1}) of $M(PMe_3)_4H_2[\eta^2\text{-}OC_6H_2Me_2(CH_2)]$ relative to $M(PMe_3)_4(OC_6H_2Me_3)H$ (M = Mo, W)

	Mo	W
$M(PMe_3)_4(OC_6H_2Me_3)H$	0	0
$M(PMe_3)_4H_2(\eta^2\text{-}OC_6H_2Me_2CH_2)$	+5.9	−6.0

In order to assess the validity of the calculations on $M(PMe_3)_4(OC_6H_2Me_3)H$ and $M(PMe_3)_4H_2[(\eta^2\text{-}OC_6H_2Me_2(CH_2)]$, DFT studies were also performed on $M(PMe_3)_6$ and $M(PMe_3)_4(\eta^2\text{-}CH_2PMe_2)H$ (M = Mo, W), which represent a related system in which experimental values for ΔH have been measured. The results are shown in Table 7, from which it can be seen that the calculated energies for the cyclometallation of $M(PMe_3)_6$ are significantly less than the experimental values, such that the reaction is predicted to be exothermic, whereas experimentally, ΔH was found to be positive. The calculations do, however, reproduce the result that formation of $M(PMe_3)_4(\eta^2\text{-}CH_2PMe_2)H$ is more favored for W than for Mo, by ca. 9 kcal mol^{-1}, compared with the measured difference of 6.6 kcal mol^{-1}. It should be noted, however, that the formation of $M(PMe_3)_4(\eta^2\text{-}CH_2PMe_2)H$ also involves dissociation of a phosphine ligand from $M(PMe_3)_6$ and so is not a direct measure of the difference in M–H and M–C bond strengths.

Table 7
Calculated and experimental energies (kcal mol^{-1}) for cyclometallation of $M(PMe_3)_6$

	Mo	W	Mo–W
ΔH (experimental)	15.9 [a]	9.3 [b]	6.6
ΔE (calculated)	−1.3	−10.7	9.4

[a] V.J. Murphy, G. Parkin, J. Am. Chem. Soc. 117 (1995) 3522–3528.
[b] D. Rabinovich, R. Zelman, G. Parkin, J. Am. Chem. Soc. 114 (1992), 4611–4621.

2.4. Oxidative addition of H_2 to $Mo(PMe_3)_4(OC_6H_2Me_3)H$ and reductive elimination of ArOH

A further distinction between the molybdenum and tungsten systems is that the tungsten compound $W(PMe_3)_4H_2[\eta^2\text{-}OC_6H_2Me_2(CH_2)]$ is stable to H_2 at 110 °C [3], whereas at 80 °C $Mo(PMe_3)_4(OC_6H_2Me_3)H$ liberates the phenol $C_6H_2Me_3OH$ and forms $Mo(PMe_3)_4H_4$ (Scheme 8). Likewise, $Mo(PMe_3)_4(OC_6H_3Pr^i_2)H$ reacts with H_2 to give $Mo(PMe_3)_4H_4$ and $C_6H_3Pr^i_2OH$. The reaction between $Mo(PMe_3)_4(OAr)H$ and H_2 is postulated to occur via initial oxidative addition and formation of $Mo(PMe_3)_4(OAr)H_3$. Support for this proposal is not only provided by the fact that several analogous tungsten complexes $W(PMe_3)_4(OAr)H_3$ have been reported [3], but also by deuterium labeling and magnetization transfer experiments. For example, treatment of $Mo(PMe_3)_4(OC_6H_2Me_3)H$ with D_2 at room temperature results in deuterium incorporation into both the *ortho*-methyl groups and the hydride sites, as judged by ^{1}H-NMR and ^{2}H-NMR spectroscopy. More interestingly, magnetization transfer is observed between the resonances of the *ortho*-methyl groups, the hydride and dissolved H_2, indicating that all three types of hydrogen exchange with each other rapidly on the NMR timescale [34]. However, due to the competing rapid exchange between three sites, quantitative rate information was not extracted from the magnetization transfer experiment. The deuterium labeling and magnetization transfer studies are consistent with the mechanism illustrated in Scheme 9.

In a similar fashion, deuterium labeling studies also demonstrate that both types of C–H bonds (methyl and methine) of the *ortho*-isopropyl substituents of $Mo(PMe_3)_4(OC_6H_3Pr^i_2)H$ undergo reversible activation in the presence of D_2, prior to reductive elimination of $C_6H_3Pr^i_2OH$ and formation of $Mo(PMe_3)_4H_4$. Magnetization transfer studies indicate that exchange between H_2 and the hydride sites occurs rapidly at room temperature. Since exchange with the isopropyl hydrogens does not occur at room temperature, it permits determination of the rate constant for oxidative addition of H_2 (6.2 M^{-1} s^{-1} at 303 K) [25].

3. Experimental

3.1. General considerations

All manipulations were performed using a combination of glovebox, high-vacuum or Schlenk techniques [35]. Solvents were purified and degassed by standard procedures and all commercially available reagents were used as received, unless otherwise noted in the experi-

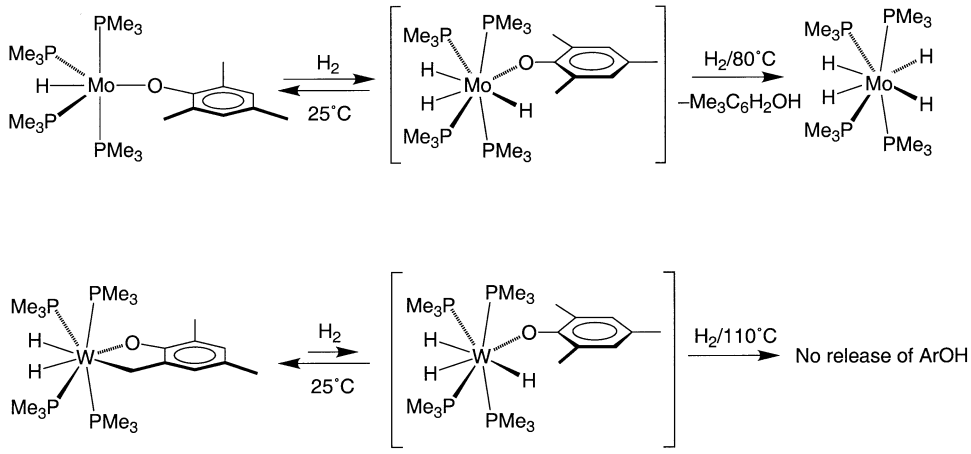

Scheme 8.

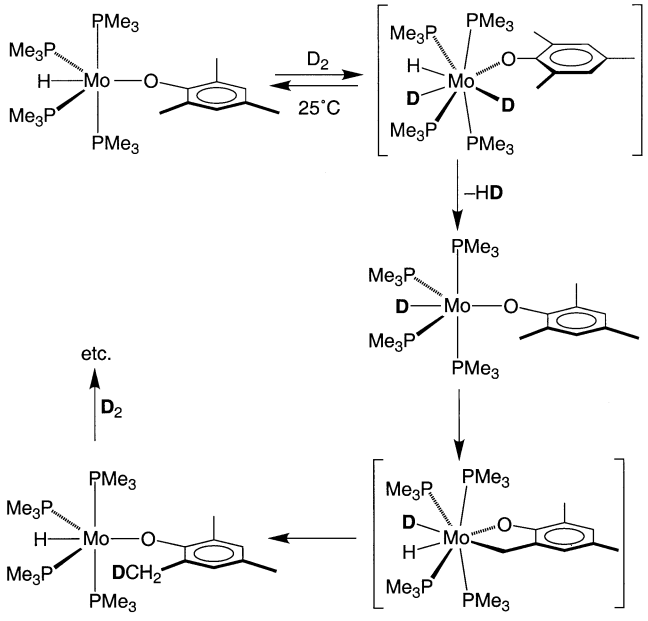

Scheme 9.

mental procedures. IR spectra were recorded as KBr pellets or neat samples on Perkin–Elmer 1430 or 1600 spectrophotometers and are reported in cm^{-1}. Elemental analyses were measured using a Perkin–Elmer 2400 CHN Elemental Analyzer. ^{1}H-NMR spectra were recorded on Varian VXR-200 (200.057 MHz), VXR-300 (299.943 MHz), VXR-400 (399.95 MHz) and Bruker Avance DPX 300, DRX 300 and DMX 500 spectrometers. ^{1}H and ^{13}C chemical shifts are reported in ppm relative to $SiMe_4$ ($\delta = 0$) and were referenced internally with respect to the protio solvent impurity ($\delta = 7.15$ for C_6D_5H) and the ^{13}C resonances ($\delta = 128.0$ for C_6D_6), respectively. ^{31}P-NMR chemical shifts are reported in ppm relative to 85% H_3PO_4 ($\delta = 0$) and were referenced using $P(OMe_3)$ ($\delta = 141.0$) as external standard. $Mo(PMe_3)_6$ was prepared by the literature method [5a] and all manipulations of it were performed under an argon atmosphere.

3.2. Synthesis of $Mo(PMe_3)_4H_2(\eta^2\text{-}CH_2O)$

A suspension of $Mo(PMe_3)_6$ (0.43 g, 0.78 mmol) in pentane (25 ml) was treated with excess methanol (0.9 ml, 22 mmol). The reaction was stirred at room temperature (r.t.) overnight, yielding a golden-brown solution. The volatile components were then removed under reduced pressure, the residue extracted into pentane (20 ml), filtered, and the pentane removed under vacuum, yielding $Mo(PMe_3)_4H_2(\eta^2\text{-}CH_2O)$ as a brown solid (0.21 g, 62%). ^{1}H-NMR (C_6D_6): 3.51 [s, CH_2O], 1.20 [s, 4 $P(CH_3)_3$], −2.65 [quint, $J_{P-H} = 38$, 2 MoH]. ^{13}C-NMR (C_6D_6): 63.4 [t, $J_{P-C} = 6$; t, $J_{C-H} = 159$; CH_2O], 22.6 [br m, 4 $P(CH_3)_3$]. ^{31}P-NMR (C_6D_6): 3.5 [br s]. Anal. Calc. for $C_{13}H_{40}OP_4Mo$: C, 36.1; H, 9.3%. Found: C, 35.5; H, 9.3%. IR data (KBr, cm^{-1}): 2965 (m), 2902 (m), 2807 (w), 1734 (m), 1420 (m), 1294 (m), 1276 (m), 1153 (m), 937 (s), 845 (m), 696 (m).

3.3. Synthesis of $Mo(PMe_3)_2(OPh)_4$

A mixture of $Mo(PMe_3)_6$ (0.69 g, 1.25 mmol) and phenol (1.00 g, 11.3 mmol) was stirred in benzene (15 ml) for 2 h. The volatile components were removed under reduced pressure and the resulting tan solid washed with pentane (3×50 ml) to give $Mo(PMe_3)_2(OPh)_4$ as an orange solid (0.33 g, 43%). ^{1}H-NMR (C_6D_6): 20.3, [s, OC_6H_5], −17 [br s, 2 $P(CH_3)_3$], −18 [br s, OC_6H_5], −22 [br s, OC_6H_5]. Anal. Calc. for $C_{30}H_{38}O_4P_2Mo$: C, 58.1; H, 6.2%. Found: C, 58.2; H, 6.0%. IR Data (KBr, cm^{-1}): 3058 (w), 2905 (w), 1583 (s), 1478 (s), 1416 (w), 1252 (s), 1157 (m), 1065 (w), 1019 (w), 994 (w), 948 (m), 854 (s), 754 (m), 694 (m), 624 (m), 603 (m), 514 (w), 462 (m).

3.4. Synthesis of $Mo(PMe_3)_4(OC_6H_2Me_3)H$

A mixture of $Mo(PMe_3)_6$ (0.38 g, 0.69 mmol) and 2,4,6-trimethylphenol (0.078 g, 0.57 mmol) in benzene (5 ml) was stirred for 1 h at 80 °C, over which period a deep purple solution was obtained. The volatile components were removed under reduced pressure and the residue was extracted into pentane (ca. 20 ml). The filtrate was concentrated to ca. 5 ml and cooled to −78 °C, giving $Mo(PMe_3)_4(OC_6H_2Me_3)H$ as a purple crystalline solid which was isolated by filtration and dried in vacuo (0.16 g); further concentration of the filtrate followed by storage at −78 °C yielded an additional 0.02 g. Total yield: 0.18 g (59% based on ArOH). ^{1}H-NMR (C_6D_6): 6.99 [s, $OC_6\underline{H}_2Me_3$], 2.35 [s, *para*-$C\underline{H}_3$], 2.08 [2 *ortho*-$C\underline{H}_3$], 1.37 [s, 2 $P(C\underline{H}_3)_3$], 1.01 [s, 2 $P(C\underline{H}_3)_3$], −6.59 [t, $J_{P-H} = 23$; t, $J_{P-H} = 84$; $Mo\underline{H}$]. ^{13}C-NMR (C_6D_6): 167.3 [s, $O\underline{C}_6H_2Me_3$], 129.0 [d, $J_{C-H} = 150$, $O\underline{C}_6H_2Me_3$], 121.9 [s, $O\underline{C}_6H_2Me_3$], 121.1 [s, $O\underline{C}_6H_2Me_3$], 30.9 [d, $J_{P-C} = 17$; q, $J_{C-H} = 129$; 2 $P(C\underline{H}_3)_3$], 21.3 [q, $J_{C-H} = 128$; 2 $P(C\underline{H}_3)_3$], 21.0 [q, $J_{C-H} = 128$; 2 *ortho*-$\underline{C}H_3$], 17.7 [q, $J_{C-H} = 128$; *para*-$\underline{C}H_3$]. ^{31}P{^{1}H, $P(C\underline{H}_3)_3$} NMR (C_6D_6): 45.6 [t, $J_{P-P} = 23$; d, $J_{P-H} = 84$, 2 $\underline{P}(CH_3)_3$], 1.01 [t, $J_{P-P} = 23$; d, $J_{P-H} = 23$, 2 $\underline{P}(CH_3)_3$]. Anal. Calc. for $C_{21}H_{48}OP_4Mo$: C, 47.0; H, 9.0%. Found: C, 46.9; H, 9.0%. IR Data (KBr, cm^{-1}): 2964 (m), 2900 (m), 1750 (w) [ν_{Mo-H}], 1603 (w), 1472 (m), 1421 (m), 1369 (w), 1312 (m), 1292 (m), 1269 (m), 1156 (w), 934 (s), 847 (m), 821 (m), 734 (m), 696 (m), 676 (m), 645 (m), 509 (m). The reaction of $Mo(PMe_3)_6$ with $C_6H_2Me_3OD$ [36] was monitored by both ^{1}H and ^{2}H-NMR spectroscopy.

3.5. Synthesis of $Mo(PMe_3)_4(OC_6H_3Pr^i_2)H$

A mixture of $Mo(PMe_3)_6$ (0.44 g, 0.80 mmol) and 2,6-diisopropylphenol (0.13 ml, 0.70 mmol) in benzene (5 ml) was stirred for 1.5 h at 60 °C, over which period a deep purple solution was obtained. The volatile components were removed under reduced pressure and the residue extracted into pentane (ca. 20 ml). The filtrate was concentrated to ca. 2 ml and cooled to −78 °C, giving $Mo(PMe_3)_4(OC_6H_3Pr^i_2)H$ as a purple crystalline solid which was isolated by filtration and dried in vacuo. Yield: 0.24 g (59% based on ArOH). ^{1}H-NMR (C_6D_6): 7.21 [d, $J_{H-H} = 7.5$, 2 *meta*-H], 6.86 [t, $J_{H-H} = 7.5$, *para*-H], 3.22 [septet, $J_{H-H} = 7$, 2 $C\underline{H}(CH_3)_2$], 1.39 [d, $J_{P-H} = 14$, 2 $P(C\underline{H}_3)_3$], 1.37 [d, $J_{H-H} = 7$, 2 $CH(C\underline{H}_3)_2$], 1.00 [s, 2 $P(C\underline{H}_3)_3$], −6.53 [t, $J_{P-H} = 22$; t, $J_{P-H} = 85$; $Mo\underline{H}$]. ^{13}C-NMR (C_6D_6): 167.5 [s, $O\underline{C}_6H_3Pr^i_2$], 133.5 [s, $O\underline{C}_6H_3Pr^i_2$], 122.5 [d, $J_{C-H} = 150$, $O\underline{C}_6H_3Pr^i_2$], 114.7 [d, $J_{C-H} = 157$, $O\underline{C}_6H_3Pr^i_2$], 30.5 [q, $J_{C-H} = 127$; d, $J_{P-C} = 18$; 2 $P(\underline{C}H_3)_3$], 25.7 [d, $J_{C-H} = 125$, 2 $\underline{C}H(CH_3)_2$], 24.9 [q, $J_{C-H} = 125$, 2 $CH(\underline{C}H_3)_2$], 22.4 [q, $J_{C-H} = 126$, 2 $P(\underline{C}H_3)_3$]. ^{31}P{^{1}H, $P(C\underline{H}_3)_3$} NMR (C_6D_6): 48.3 [t, $J_{P-P} = 23$; d, $J_{P-H} = 85$, 2 $\underline{P}(CH_3)_3$], 1.13 [t, $J_{P-P} = 23$; d, $J_{P-H} = 223$, 2 $\underline{P}(CH_3)_3$]. Anal. Calc. for $C_{24}H_{54}OP_4Mo$: C, 49.8; H, 9.4%. Found: C, 49.8; H, 9.3%. IR Data (KBr, cm^{-1}): 2964 (m), 2903 (m), 1751 (w) [ν_{Mo-H}], 1585 (m), 1425 (m), 1337 (m), 1274 (m), 1108 (w), 1044 (w), 930 (s), 740 (m), 692 (m), 643 (m).

Table 8
Crystal, intensity collection and refinement data

	$Mo(PMe_3)_4H_2(\eta^2\text{-}CH_2O)$	$Mo(PMe_3)_2(OPh)_4$	$Mo(PMe_3)_4(OC_6H_2Me_3)H$	$Mo(PMe_3)_4(OC_6H_3Pr^i_2)H$
Lattice	Monoclinic	Monoclinic	Triclinic	Orthorhombic
Formula	$C_{13}H_{40}MoOP_4$	$C_{30}H_{38}MoOP_4$	$C_{21}H_{48}MoOP_4$	$C_{24}H_{54}MoOP_4$
Formula weight	432.27	620.5	536.4	578.5
Space group	$P2/c$	$P2_1/c$	$P\bar{1}$	*Pnma*
a (Å)	16.4296(15)	10.212(2)	9.514(2)	20.055(5)
b (Å)	9.6195(9)	10.606(3)	12.220(2)	17.076(5)
c (Å)	15.7796(15)	14.607(2)	12.820(3)	9.400(3)
α (°)	90	90	87.24(2)	90
β (°)	117.756(2)	98.11(2)	77.80(2)	90
γ (°)	90	90	81.99(2)	90
V (Å^3)	2206.9(4)	1567.5(8)	1442.3(5)	3219.0(16)
Z	4	2	2	4
Temperature (K)	223	295	295	295
Radiation (λ, Å)	0.71073	0.71073	0.71073	0.71073
ρ_{calc} (g cm^{-3})	1.301	1.315	1.235	1.194
μ (Mo–K$_\alpha$), (mm^{-1})	0.878	0.551	0.686	0.619
θ_{max} (°)	28.3	22.5	25.0	22.5
Number of data	5122	2045	3226	2934
Number of parameters	216	170	249	152
R_1	0.0427	0.0378	0.0327	0.0544
wR_2	0.0812	0.0522	0.0428	0.0606

3.6. Computational details

All DFT calculations were performed using Jaguar [37]. Geometries were optimized starting from the X-ray crystal structure coordinates of $Mo(PMe_3)_4(OC_6H_2Me_3)H$, $W(PMe_3)_4H_2[\eta^2\text{-}OC_6H_2Me_2(CH_2)]$, $W(PMe_3)_6$ and $W(PMe_3)_4(\eta^2\text{-}CH_2PMe_2)H$ at the BLYP level using the LACVP** basis set. No symmetry constraints were used. The structures of $M(PMe_3)_6$ (M = Mo, W) converged to S_6 symmetry and those of $M(PMe_3)_4(\eta^2\text{-}CH_2PMe_2)H$ (M = Mo, W) converged to C_s symmetry. Single point energy calculations were then performed on the optimized structures with appropriate symmetry constraints at the B3LYP level using triple-ζ basis sets (LACV3P** for the transition metals, cc-pVTZ(-f) for all other elements). PMe_3 was optimized at the B3LYP level with the cc-pVTZ(-f) basis set.

3.7. X-ray structure determinations

X-ray diffraction data for $Mo(PMe_3)_4H_2(\eta^2\text{-}CH_2O)$ were collected on a Bruker P4 diffractometer equipped with a SMART CCD detector; data for all other complexes were collected using a Siemens P4 diffractometer. Crystal data, data collection and refinement parameters are summarized in Table 8. The structures were solved using direct methods and standard difference map techniques, and were refined by full-matrix least-squares procedures using SHELXTL [38]. Hydrogen atoms on carbon were included in calculated positions.

4. Summary

In summary, $Mo(PMe_3)_6$ reacts with methanol to give the formaldehyde complex $Mo(PMe_3)_4(\eta^2\text{-}CH_2O)$, analogous to that of the tungsten system, whereas the reactions with phenol and its derivatives yield significantly different products. Specifically, the tendency to achieve C–H bond activation for a molybdenum center is reduced considerably from that for a tungsten center, so that the products of the molybdenum system are simple aryloxy derivatives, e.g. $Mo(PMe_3)_2(OPh)_4$ and $Mo(PMe_3)_4(OAr)H$, whereas cyclometalated C–H cleavage products, e.g. $W(PMe_3)_4(\eta^2\text{-}OC_6H_4)H_2$ and $W(PMe_3)_4[\eta^2\text{-}OC_6H_2Me_2(CH_2)]H_2$, are obtained for the tungsten system. Such differences are attributed to weaker M–C and M–H bond energies for molybdenum compared with tungsten, such that the C–H bond activation products are thermodynamically unstable. Despite this instability, deuterium labeling and magnetization transfer studies demonstrate that the coordinatively unsaturated molybdenum complexes $Mo(PMe_3)_4(OAr)H$ are nevertheless kinetically capable of intramolecular C–H bond activation.

5. Supplementary material

The crystallographic data for $Mo(PMe_3)_4H_2(\eta^2\text{-}CH_2O)$ (CCDC 173846), $Mo(PMe_3)_2(OPh)_4$ (CCDC TORDIN), $Mo(PMe_3)_4(OC_6H_2Me_3)H$ (CCDC TORDOT), and $Mo(PMe_3)_4(OC_6H_3Pr^i_2)H$ (CCDC TORDUZ) have been deposited with the Cambridge Crystallographic Data Center. Copies of this information may be obtained free of charge from The Director, CCDC, 12 Union Road, Cambridge CB2 1EZ, UK (Fax: +44-1223-336033; e-mail: deposit@ccdc.cam.ac.uk or www: http://www.ccdc.cam.ac.uk).

Acknowledgements

We thank the US Department of Energy, Office of Basic Energy Sciences (#DE-FG02-93ER14339) for support of this research.

References

[1] (a) C.L. Hill (Ed.),Activation and Functionalization of Alkanes, Wiley, New York 1989;
(b) B.A. Arndtsen, R.G. Bergman, T.A. Mobley, T.H. Peterson, Acc. Chem. Res. 28 (1995) 154;
(c) A.D. Ryabov, Chem. Rev. 90 (1990) 403;
(d) W.D. Jones, F.J. Feher, Acc. Chem. Res. 22 (1989) 91;
(e) Special issue J. Organomet. Chem. 504 (1996).;
(f) A.E. Shilov, G.B. Shul'pin, Chem. Rev. 97 (1997) 2879;
(g) R.H. Crabtree, J. Chem. Soc. Dalton Trans. (2001) 2437.

[2] M.L.H. Green, G. Parkin, K.J. Moynihan, K. Prout, J. Chem. Soc. Chem. Commun. (1984) 1540.

[3] (a) D. Rabinovich, R. Zelman, G. Parkin, J. Am. Chem. Soc. 112 (1990) 9632;
(b) D. Rabinovich, R. Zelman, G. Parkin, J. Am. Chem. Soc. 114 (1992) 4611.

[4] The reactivity of related tungsten complexes towards alcohols has been reported, but C–H bond activation reactions have not been observed. For example (a) $W(PMe_3)_4Cl_2$ and $W(PMe_3)_4H_2Cl_2$ react with alcohols to yield $W(PMe_3)_3(O)Cl_2$ and liberate the hydrocarbon, (b) while $W(PMe_3)_5H_2$ reacts with $PhCH_2OH$ to yield $W(PMe_3)_4H_3(OCH_2Ph)$, thermolysis of which yields $W(PMe_3)_4(CO)H_2$ and benzene. (a) T.J. Crevier, J.M. Mayer, J. Am. Chem. Soc. 119 (1997) 8485.(b) T.J. Crevier, J.M. Mayer, Inorg. Chim. Acta 270 (1998) 202.

[5] (a) V.J. Murphy, G. Parkin, J. Am. Chem. Soc. 117 (1995) 3522;
(b) M. Brookhart, K. Cox, F.G.N. Cloke, J.C. Green, M.L.H. Green, P.M. Hare, J. Bashkin, A.E. Derome, P.D. Grebenik, J. Chem. Soc. Dalton Trans. (1985) 423.

[6] Some of this work has been communicated: T. Hascall, V.J. Murphy, G. Parkin, Organometallics 15 (1996) 3910.

[7] M. Minato, H. Sakai, Z.-G. Weng, D.-Y. Zhou, S. Kurishima, T. Ito, M. Yamasaki, M. Shiro, M. Tanaka, K. Osakada, Organometallics 15 (1996) 4863.

[8] Furthermore, $Cp_2Mo(\eta^2\text{-}CH_2O)$ has been reported. See: (a) G.E. Herbereich, J. Okuda, Angew. Chem. Int. Ed. Engl. 24 (1985) 402.(b) S. Gambarotta, C. Floriani, A. Chiesi-Villa, C. Guastini, J. Am. Chem. Soc. 107 (1985) 2985.

[9] The triplet is further split into a triplet of triplets due to coupling to phosphorus.
[10] Interestingly, both paramagnetic and diamagnetic tungsten(IV) complexes of the type $W(PR_3)_2(OAr)_2X_2$ are known, depending on the nature of the substituents. See: (a) L.M. Atagi, J.M. Mayer, Angew. Chem. Int. Ed. Engl. 32 (1993) 439.(b) C.E. Kriley, P.E. Fanwick, I.P. Rothwell, J. Am. Chem. Soc. 116 (1994) 5225.(c) J.L. Kerschner, P.E. Fanwick, I.P. Rothwell, J.C. Huffman, Inorg. Chem. 28 (1989) 780.
[11] S. Jang, L.M. Atagi, J.M. Mayer, J. Am. Chem. Soc. 112 (1990) 6413.
[12] T. Hascall, G. Parkin, unpublished results.
[13] (a) J.L. Kerschner, P.E. Fanwick, I.P. Rothwell, J. Am. Chem. Soc. 109 (1987) 5840;
(b) J.L. Kerschner, P.E. Fanwick, I.P. Rothwell, J.C. Huffman, Organometallics 8 (1989) 1424.
[14] (a) K. Osakada, K. Ohshiro, A. Yamamoto, Organometallics 10 (1991) 404;
(b) J.F. Hartwig, R.A. Andersen, R.G. Bergman, Organometallics 10 (1991) 1875;
(c) M.J. Burn, M.G. Fickes, F.J. Hollander, R.G. Bergman, Organometallics 14 (1995) 137.
[15] For some other structurally characterized transition metal aryloxy-hydride complexes containing phosphine ligands, see: (a) J.R. Bleeke, T. Haile, P.R. New, M.Y. Chiang, Organometallics 12 (1993) 517.(b) A.L. Seligson, R.L. Cowan, W.C. Trogler, Inorg. Chem. 30 (1991) 3371.(c) R.L. Cowan, W.C. Trogler, J. Am. Chem. Soc. 111 (1989) 4750.(d) F.T. Ladipo, M. Kooti, J.S. Merola, Inorg. Chem. 32 (1993) 1681.(e) B.C. Ankianiec, P.E. Fanwick, I.P. Rothwell, J. Am. Chem. Soc. 113 (1991) 4710.(f) V.M. Visciglio, P.E. Fanwick, I.P. Rothwell, J. Chem. Soc. Chem. Commun. (1992) 1505.(g) C. Di Bugno, M. Pasquali, P. Leoni, P. Sabatino, D. Braga, Inorg. Chem. 28 (1989) 1390.(h) H. Nöth, M. Schmidt, Organometallics 14 (1995) 4601.
[16] D. Milstein, J.C. Calabrese, I.D. Williams, J. Am. Chem. Soc. 108 (1986) 6387.
[17] The structure is fluxional on the NMR time-scale and the hydride resonance appears as a quintet with $J_{P-H} = 47$ Hz. See: R.A. Henderson, D.L. Hughes, R.L. Richards, C. Shortman, J. Chem. Soc. Dalton Trans. (1987) 1115.
[18] T. Hascall, D. Rabinovich, V.J. Murphy, M.D. Beachy, R.A. Friesner, G. Parkin, J. Am. Chem. Soc. 121 (1999) 11402.
[19] Furthermore, the departure from octahedral symmetry of $Mo(PMe_3)_4(OAr)H$ also promotes the selective π-interaction with a single metal orbital.
[20] (a) J.L. Kerschner, P.E. Fanwick, I.P. Rothwell, Inorg. Chem. 28 (1989) 780;
(b) W.A. Howard, T.M. Trnka, G. Parkin, Inorg. Chem. 34 (1995) 5900;
(c) B.D. Steffey, P.E. Fanwick, I.P. Rothwell, Polyhedron 9 (1990) 963;
(d) T.W. Coffindaffer, B.D. Steffy, I.P. Rothwell, K. Folting, J.C. Huffman, W.E. Streib, J. Am. Chem. Soc. 111 (1989) 4742.
[21] It should be noted that deuterium incorporation is also observed in the PMe_3 resonances of $Mo(PMe_3)_4(OC_6H_2Me_3)H$. In this regard, the reaction of $W(PMe_3)_4(\eta^2\text{-}CH_2PMe_2)H$ with C_6H_5OD results in deuterium incorporation into the PMe_3 groups of $W(PMe_3)_4H_2(\eta^2\text{-}OC_6H_4)$ as well as in the free phosphine liberated in the reaction. This observation was explained by a mechanism involving a direct attack by phenol of the W–C bond of $W(PMe_3)_4(\eta^2\text{-}CH_2PMe_2)H$ (reference [3]). Thus deuterium incorporation into the PMe_3 ligands of $Mo(PMe_3)_4(OC_6H_2Me_3)H$ suggests a competitive mechanism involving reaction of $W(PMe_3)_4(\eta^2\text{-}CH_2PMe_2)H$ with the phenol.
[22] It is, of course, possible that the six-coordinate complexes $Mo(PMe_3)_4(OAr)H$ may dissociate PMe_3 prior to the C–H bond activation step, cf. the mechanism for oxidative-addition of H_2 to $W(PMe_3)_4I_2$. See: D. Rabinovich, G. Parkin, J. Am. Chem. Soc. 115 (1993) 353.
[23] (a) R. Freeman, A Handbook of Nuclear Magnetic Resonance, Longman, Harlow, UK 1988;
(b) D.C. Roe, P.M. Kating, P.J. Krusic, B.E. Smart, Top. Catal. 5 (1998) 133.
[24] Exchange between the two PMe_3 ligands of $Mo(PMe_3)_4(OC_6H_2Me_3)H$ and free PMe_3 was also observed by magnetization transfer experiments. The PMe_3 exchange, however, appears to be independent from the cyclometallation as the rate of the hydride/*ortho*-methyl exchange was not noticeably affected by the presence of added PMe_3.
[25] It is important to note that appropriate statistical factors have been included in order to relate the observed magnetization transfer rate constants to those of the actual chemical processes involved. See, for example: M.L.H. Green, L.-L. Wong, A. Sella, Organometallics 11 (1992) 2660.
[26] (a) T.J. Marks (Ed.), Bonding Energetics in Organometallic Compounds, ACS Symposium Series, 1990, pp. 428;
(b) J.A. Martinho Simões, J.L. Beauchamp, Chem. Rev. 90 (1990) 629;
(c) D.C. Eisenberg, J.R. Norton, Israel J. Chem. 31 (1991) 55;
(d) H.A. Skinner, J.A. Connor, Pure Appl. Chem. 57 (1985) 79;
(e) J.A. Martinho Simões (Ed.), Energetics of Organometallic Species, NATO ASI series, 1991, pp. 367;
(f) Halpern, J. Acc. Chem. Res. 15 (1982) 238.
[27] It must also be recognized that the oxidative-addition of the C–H bond will be accompanied by loss of oxygen to metal π-donation.
[28] For another example in which intramolecular C–H bond activation is observed in a dinuclear tungsten complex, but not in the analogous Mo species, see: M.H. Chisholm, J.-H. Huang, J.C. Huffman, I.P. Parkin, Inorg. Chem. 36 (1997) 1642.
[29] (a) M.J. Calhorda, A.R. Dias, M.E. Minas da Piedade, M.S. Salema, J.A. Martinho Simões, Organometallics 6 (1987) 734;
(b) A.R. Dias, J.A. Martinho Simões, Polyhedron 7 (1988) 1531.
[30] See for example, reference [18].
[31] The electronic energies are the enthalpies at 0 K uncorrected for zero point energy contributions.
[32] D.F. McMillen, D.M. Golden, Ann. Rev. Phys. Chem. 33 (1982) 493.
[33] It is worth noting that the sum of the M–C and M–H bond energies for the Mo and W complexes is significantly less for $Mo(PMe_3)_4H_2[\eta^2\text{-}OC_6H_2Me_2(CH_2)]$ than those for the Cp_2MX_2 system. In part, this difference may be attributed to a more crowded environment in the former system.
[34] For some other examples of magnetization transfer between H_2 and hydride ligands, see: (a) B.E. Hauger, D. Gusev, K.G. Caulton, J. Am. Chem. Soc. 116 (1994) 208.(b) R.L. Miller, R. Toreki, R.E. LaPointe, P.T. Wolczanski, G.D. Van Duyne, D.C. Roe, J. Am. Chem. Soc. 115 (1993) 5570.(c) J. Halpern, L. Cai, P.J. Desrosiers, Z. Lin, J. Chem. Soc. Dalton Trans. (1991) 717.
[35] (a) J.P. McNally, V.S. Leong, N.J. Cooper, in: A.L. Wayda, M.Y. Darensbourg (Eds.), Experimental Organometallic Chemistry (chapter 2), American Chemical Society, Washington, DC 1987, pp. 6–23;
(b) B.J. Burger, J.E. Bercaw, in: A.L. Wayda, M.Y. Darensbourg (Eds.), Experimental Organometallic Chemistry (chapter 4), American Chemical Society, Washington, DC 1987, pp. 79–98;
(c) D.F. Shriver, M.A. Drezdzon, The Manipulation of Air-Sensitive Compounds, 2nd ed., Wiley-Interscience, New York 1986.
[36] $C_6H_2Me_3OD$ was obtained by stirring a solution of 2,4,6-trimethylphenol (0.48 g) in D_2O (4 ml) and CH_3CN (15 ml)

containing a catalytic amount of HCl (aq) overnight. The volatile components were removed in vacuo to give $C_6H_2Me_3OD$ [^{2}H-NMR (C_6H_6): δ 3.9]. Deuteration was found to be ca. 90% complete by ^{1}H-NMR spectroscopy.

[37] JAGUAR Version 3.5, Schrödinger, Inc., Portland, OR, 1998.

[38] G.M. Sheldrick, SHELXTL, An Integrated System for Solving, Refining and Displaying Crystal Structures from Diffraction Data, University of Göttingen, Göttingen, Federal Republic of Germany 1981.